Impact failure of continuous fiber reinforced Al-matrix composites subjected to low velocity impact

Ramadan J. Mustafa, Yassin L. Nimir and Mahmoud Alhusein
Dept. of Mechanical Eng., Faculty of Eng., Mu'tah University, Karak, Jordan

An investigation consisting of experiments was performed to study impact damage mechanisms of unidirectional 50% v/o SiC-Al (1050), 50% v/o SiC-Al (354) and 50% high modulus (H.M.) C-Al (356) composites subjected to low velocity impact tests. The composites were made from unidirectionally infiltrated Al-Si-Mg alloy and commercially pure Al (1050) into preforms of continuous SiC and H.M. carbon fibers with a nominal fiber diameter of 7-20 μm. A controlled drop-weight test rig was used that provided load-time and energy-time curves. SEM investigation of fracture surfaces and the results obtained show that matrix cracking is the initial failure mode of impact damage causing fiber-matrix interfacial debonding and micro-cracks. For a given composite, their exists a threshold incident energy above which a significant damage in the form of delamination crack will occur at the first impact. As a consequence, both strength and stiffness were reduced and these properties could be measured using the same impact tester as a function of number of impacts. Both the number and size of delamination and thickness-direction cracks were then found to increase as the number of impacts was increased.

تم في هذا البحث دراسة عملية على آليات تأثير الصدم بسرعات منخفضة على بعض المواد المركبة المكونة من سيليكون كاربايد –ألمنيوم (١٠٥٠)، سيليكون كاربايد – ألمنيوم (٣٥٤) وكاربون –ألمنيوم (٣٥٦). تم تصنيع هذه المواد من سبائك المواد من سبائك ألمنيوم – سيليكون مغنيسيوم وألمنيوم نقي تجاري (١٠٥٠) ومن ألياف مستمرة أحادية الاتجاه من السيليكون كاربايد وألياف من الكربون ويتراوح قطر الألياف من ٧ إلى ٢٠ ميكرون. يتكون جهاز الفحص من وزن يتم التحكم بسقوطه لكي يرتطم بالعينات المعدة من المواد المركبة الآنفة الذكر وتم الحصول على منحنيات للحمل مع الزمن والطاقة مع الزمن ومن ثم تم فحص سطوح الكسر للعينات بواسطة المجهر الإلكتروني وتم تحليل النتائج والتي أظهرت إن تفسخ مادة الترابط هو نمط الانهيار الابتدائي لهذه المواد والذي تسبب بانحلال الترابط السطحي بين الأرضية المعدنية والألياف وتصدعات صغيرة إضافية إلى نتائج متعددة أظهرتها هذه الدراسة.

Keywords: Metal matrix composites, Impact test, Incident energy, Delamination

1. Introduction

Metal matrix composites are being increasingly used as primary structural engineering components in different engineering fields due to their inherently high specific mechanical properties. In many situations, the composites are likely to encounter different kinds of impacts by foreign object projectiles during the practical manufacturing phase or in the field use. Usually, the composites are very susceptible to impact events. It has been shown by many researchers, [1-3], that low velocity impact on the composite laminates produces multiple delaminations at a number of interfaces through the thickness of composite laminates. The delaminations may cause significant strength and stiffness reductions of such laminates. The method most widely used for determining impact damage failure was the Compression-After-Impact tests (CAI) [3, 4]. The difficulty and the high cost involved in performing CAI tests on the continuous fiber reinforced metal matrix composites have been well recognized.

The main aim of this research is to develop a reliable method for investigating and characterizing impact damage growth of continuous fiber reinforced metal matrix composites. This method involves repeated instrumental low-velocity impact testing of the same specimen using the same tester. In each impact event, load-time and energy-time traces, along with other numerical data on composite material properties, can be stored and analyzed by a personal computer. A similar technique has been successfully applied to measure the toughness of the unreinforced materials [5].

Alexandria Engineering Journal Vol. 41 (2002), No. 1, 47- 55
© Faculty of Engineering Alexandria University, Egypt.

In many practical situations, a composite can be subjected to repeated impacts. However, little or no work has been done in either low-velocity repeated impact testing of metal matrix composites or in the corresponding failure mechanisms. When a low-energy impact is imposed on a composite laminate, internal damage can occur as a result of the contact stresses between the impactor and the laminate. When impacts are repeated, the damage zone grows and causes a significant reduction in strength and modulus. The changes in stiffness of glass fiber reinforced polymers in tensile impact fatigue testing were measured by Prank and coworkers [6]. A life- time analysis on the impact fatigue specimens of short E-glass fiber/polyphenylene sulfide composites were developed by Lhymn [7, 8]. This current paper, however, deals with low-velocity impact failure of continuous ceramic fiber reinforced Al-matrix composites using a technique that deploys a repeated impact testing. Useful parameters have also been identified as indices for the characterization of damage tolerance of advanced composites.

2. Materials and experimental procedure

The metal matrix composites utilized in this work were manufactured by unidirectionally infiltrating Al-Si-Mg alloy (Al (354) and Al (356)) and commercially pure aluminum (1050) into preforms of Silicone Carbide (SiC) and high modulus Carbon (C) continuous fibers. The nominal fiber diameter is 7-20 μm and the fiber volume fraction (v/o) is 50%. The process of fabrication consists of cutting suitable lengths of the fiber tows, which were stacked unidirectionally and laid, in a split die. Once the fibers were in position, the die is closed and the molten metal reservoir chamber was evacuated of all air. When all parameters were fulfilled, the melt chamber was pressurized and the liquid metal was forced into the die and hence infiltrating the fibers. This unidirectional infiltration of the SiC and C fiber preforms was achieved with a type of pressure casting machine, designated a Hydrostatic Pressure Infiltration Device (HPID). The methodology of manufacturing the composite samples was adopted according to refs. [9-11].

The type and geometry of the impact test specimens were dictated by the size and the quantity of the available fabricated material plates. Therefore, using a diamond saw, the specimens with dimensions as shown in fig.1 were then cut from the unidirectional material plates. The mechanical properties of the continuous fiber reinforced aluminum matrix composites were calculated using rule of mixture for both parallel (//) and perpendicular ($\perp$) fiber directions, and then compared with experimental values obtained from ref. [12]. The mechanical properties of the composites are shown in table 1.

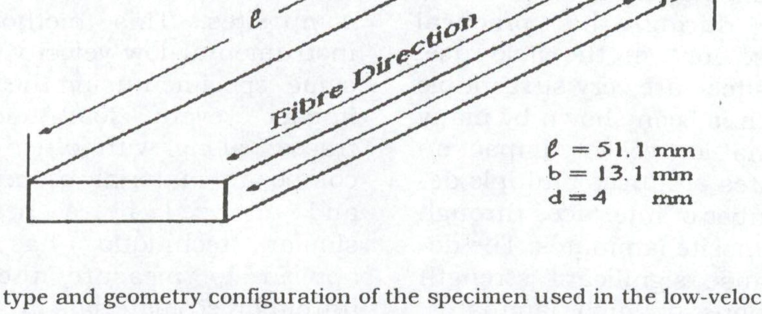

Fig. 1. The type and geometry configuration of the specimen used in the low-velocity impact tests.

Table 1
Macroscopic mechanical properties of MMC's obtained from rule of mixture, and then compared with values from ref. [12]

Composite material	Young's modulus (GPa)		Strain to failure (%)	Tensile strength MPa	
	E_{II}	$E_{\perp}$		σ_{II}	$\sigma_{\perp}$
50% v/o SiC-Al(1050)	116 115*	90	1	897	21
50% v/o SiC-Al(354)	127 128*	100	 0.27*	1026 350*	63
50%v/oH.M.C-Al(356)	152	42		285	108

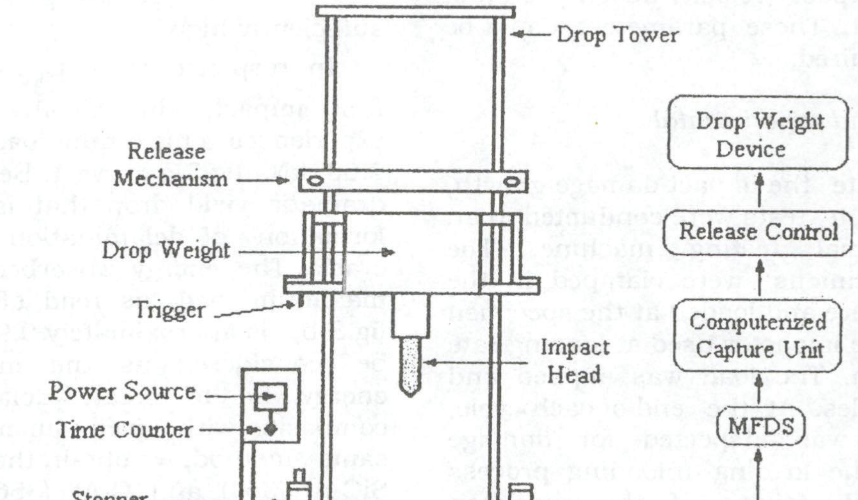

Fig. 2. Schematic diagram showing the controlled drop-weight test rig used in low-velocity tests.

2.1. Impact testing procedure

A controlled drop-weight rig shown in fig. 2 was employed to perform the impact tests A steel plate was bolted on the plat form of the test rig, and the composite specimen was clamped using 4 bolts. A load transducer is built in the impactor tip to monitor the impact response of the composite materials. The transducer signals are then transferred to a data acquisition board in an IBM PC-AT computer. This can generate, as soon as each test is conducted, plots of dynamic responses in terms of impact force as a function of time (or force-deflection curve) and energy absorbed by the specimen as a function of time (or absorbed energy-deflection). The materials characteristics obtained from the test are the maximum load, the energy at maximum load, the deflection at maximum load, the energy after maximum load (P_{max}), and the total energy absorbed. The sample is tested using a span between supports of 28-48 mm (depending on specimen thickness) with the impactor tip of 12.7 mm in diameter. The sample was then carefully placed in the same position after each test run. Here, impact energy depends on the mass and the drop height while impact velocity depends on just the drop height. These parameters could be adjusted as required.

2.2. Materials and experimental

To investigate the impact damage growth, static short-beam tests were conducted in an Instron universal testing machine. The composite specimens were clamped in the impact test fixture and loaded at the specimen center with the impactor used at loading rate of 0.4 mm/min. The load was applied and removed in cycles. At the end of each cycle, the specimen was inspected for damage assessment. The loading-unloading process continued until failure of the specimen occurred. Apparently, the damage growth within each cycle mainly occurred when the load was increased above the peak of the previous cycle. The damage accumulated at the end of each cycle was therefore equivalent to that induced by a single stroke loading to the same peak load without any intermediate loading-unloading cycles. The static short-beam observations were then used for comparison with that of impact damage assessment to elucidate the impact failure process involved.

2.3. Microscopy

The sides of composite sample specimens were metallographically polished in order to observe the microfailure mechanisms using optical and Scanning Electron Microscopes during various stages of repeated impact testing.

3. Results and discussion

The load-displacement curves for the three types of composites in response to the first impact were obtained. The acquired data also includes values of the (P^{1}_{max}), the energy absorbed up to the maximum load (E^{1}_{m}), and the elastic modulus (S^{1}). By conducting impact tests (heavy weights but low velocities) on all composites, we have found delamination would be formed in the composite if the incident energy (E_{inc}) of the first impact was sufficiently high.

In response to an E_{inc} of 2.3 J during the first impact, the SiC-Al (1050) composite experiences a maximum load at approximately 2.68 kN, fig.3-a curve 1. Beyond this comes a dramatic yield drop that is indicative of the formation of delamination (fiber debonding) crack. The energy absorbed (Em) up to this maximum load, as read of the first curve in fig.3-b, is approximately 0.95 J. This can also be considered as the minimum incident energy Ec to create delamination in the composite with given dimensions. Using the same method, we obtain the Ec values for the SiC-Al (354) and C-Al (356) composites with the same dimensions to be about 0.8 J and 0.72 J respectively. The corresponding load-time and energy-time for these materials are shown in figs. 4 and 5. The already damaged specimen(s), were impact loaded for the second time, and the load-displacement curve with numerical values of P^{2}_{max}, E^{2}_{m} and S^{2} are determined (figs 3, 4, and 5 curve 2). Here, the ratios $P^{2}_{max}/P^{1}_{max}, E^{2}_{m}/E^{1}_{m}$ and S^{2}/S^{1} may be taken as a measure for the damage failure tolerance of this composite [7]. Several curves have been plotted together on the same diagram after a number (N) of repeated impacts. As shown in figs 3 to 5, the maximum load that can be tolerated by the material decreases when the impacts are repeated. Also found to decrease is the slope of the load-time curve, which is proportional to the sample stiffness and modulus, given the same sample geometry.

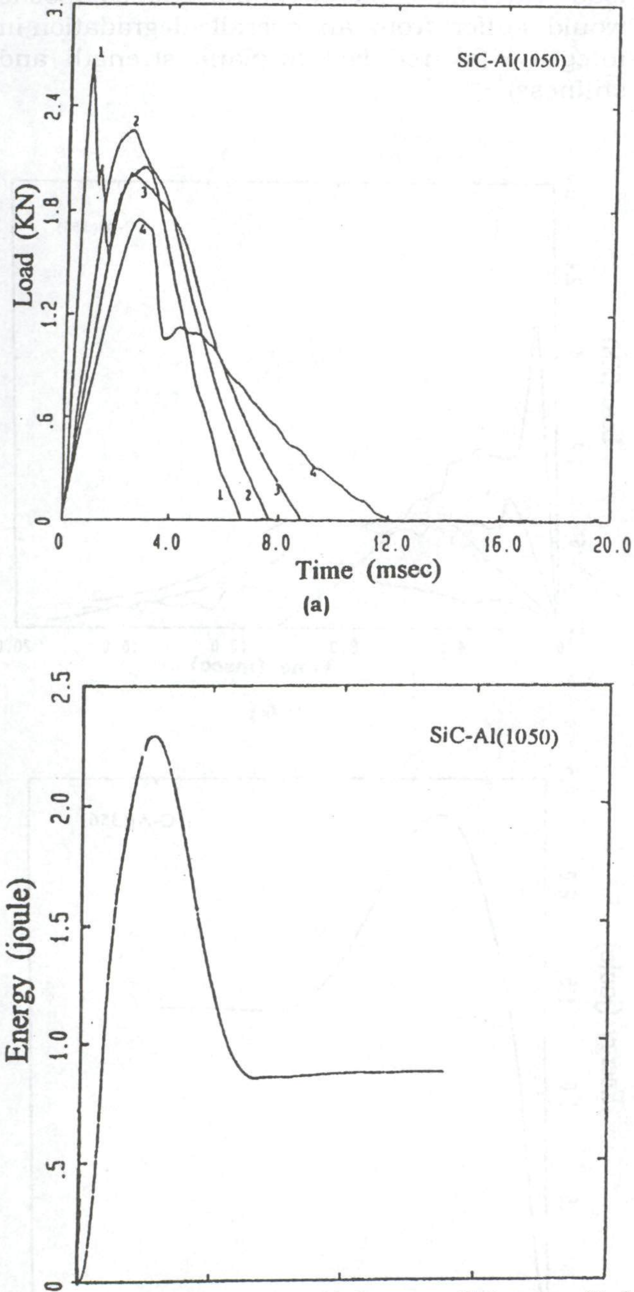

(a)

(b)

Fig. 3. (a) A number of impact (s) load-time and (b) energy-time curves for SiC- Al (1050) composites (perpendicular to fiber direction), at E_{inc} = 2.3 J.

3.1. Damage propagation and degradation diagrams

The composite damage in the first impact and impacts of the same high incident energy are repeated, the maximum load P^{N}_{max} would decrease (as seen in figs 3 to 5). The normalized strength values, $\log_{10}\left(P^{N}_{max}/P^{1}_{max}\right)$ versus $\log_{10}N$, (fig. 6-c for C-Al (356) sample) demonstrate a straight line, and the slope in the diagram is a good indication of the impact damage tolerance of the composite material, [13].

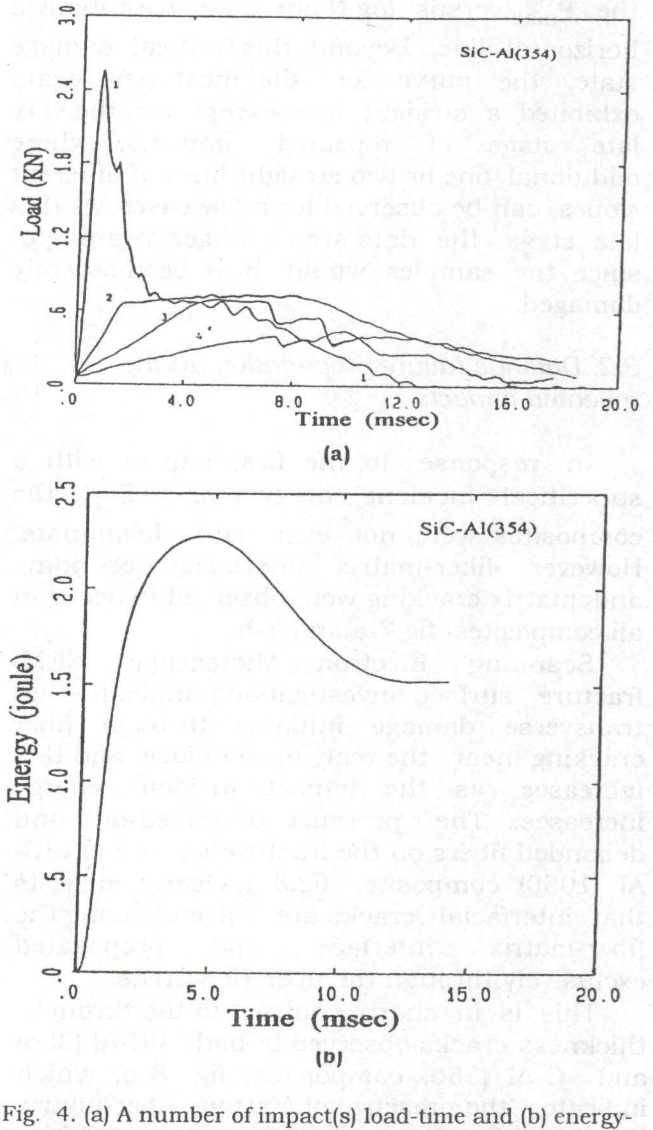

(a)

(b)

Fig. 4. (a) A number of impact(s) load-time and (b) energy-time curves for SiC- Al(354) composites (perpendicular to fiber direction), at E_{inc} = 2.3 J.

Furthermore, if the incident energy (E_{inc}) was less than Ec, no appreciable reduction in strength and stiffness was observed with the composite after several impacts. However, when the number of impacts reached a certain value (Nc) the P_{max} and the curve slope would begin to drop as N increased, as in fig. 6-a and 6-b for SiC-Al (1050) composite for an incident energy of 4.97 J and 12 J, respectively. This Nc marks a state where an appreciable level of damage is attained as usually characterized by the first observation of a few fiber-matrix interfacial debonded cracks, and can also be regarded as an indicator of the damage tolerance of a given composite. Prior to this, the P_{max}^{N} versus log N curve was essentially a horizontal line. Beyond this critical damage state, the curve for the most part again exhibited a straight line except for the very late stage of repeated impacts, where additional one or two straight lines of different slopes can be observed for a few cases. At this late stage, the data are no longer meaningful since the samples would have been severely damaged.

3.2. Damage failure propagation during repeated impacts

In response to the first impact with a subcritical incident energy ($E_{inc} < E_C$), the composites were not expected to delaminate. However, fiber-matrix interfacial debonding and matrix cracking were observed to occur in all composites, fig.7-a and 7-b.

Scanning Electron Microscope (SEM) fracture surface investigations indicate that transverse damage initiates through fiber cracking near the rear, tension face, and this increases as the impact incident energy increases. The presence of pulled-out and debonded fibers on the fracture surface of SiC-Al (1050) composite, fig.8-a, clearly suggests that interfacial cracks are deflected along the fiber-matrix interface and propagated exclusively through the fiber-rich areas.

This is in sharp contrast to the through-thickness cracks observed in both SiC-Al (354) and C-Al (356) composites, fig. 8-b, which indicates the presence of a strong fiber-matrix interfacial bonding in such composites. This is consistent with results reported by Chapman and others [11].

It is apparent that the through thickness crack extension in composites reduces it's load carrying capability, and the composite would suffer from an overall degradation in integrity (a reduced in-plane strength and stiffness).

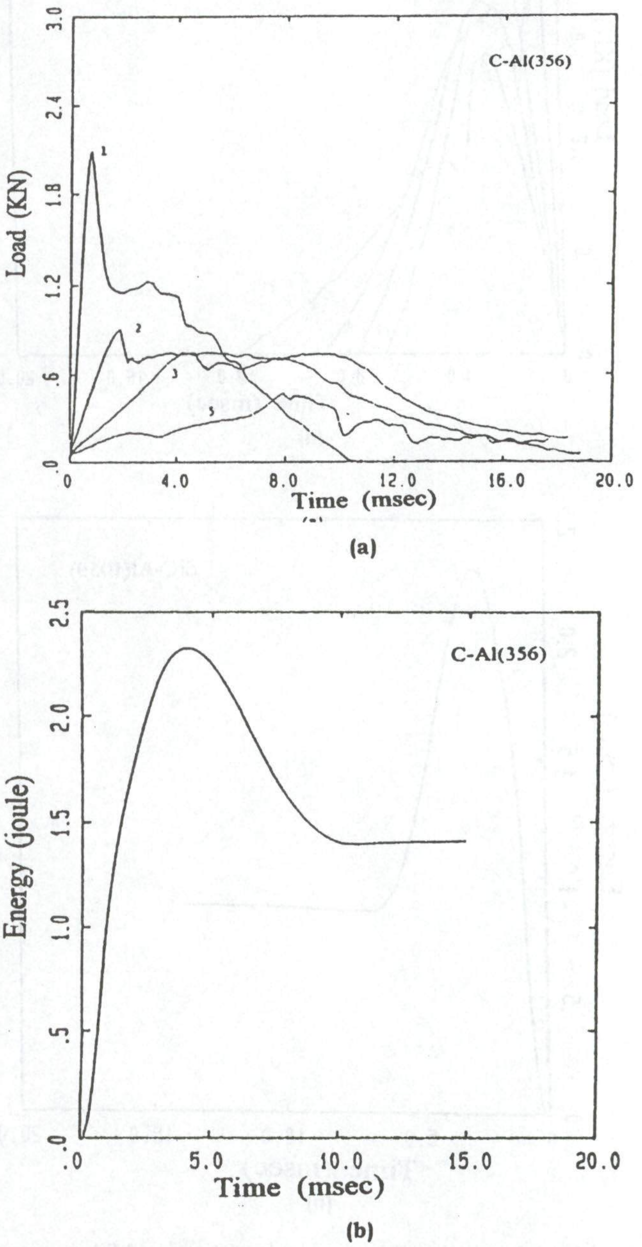

(a)

(b)

Fig. 5. (a) A number of impact (s) load-time and (b) energy-time curves for C- Al (356) composites (perpendicular to fiber direction), at E_{inc} = 2.3 J.

Studies on the matrix cracking phenomena in MMC's under tensile or cyclic stress conditions can be found in ref. [14].

It has also been observed that once the transverse cracking reaches a critical level and a delamination (i.e. interfacial debonding) crack is formed, both inplane normal strength and interlaminar shear strength are decreased. When subjected to a subsequent impact, the maximum load and the initial slope of the load-time curve will be lower than those of the first or previous impact. During each impact test, the E_{inc} must be accommodated. Part of this energy is stored and then utilized in rebounding the impactor while the rest of this energy is expected to be dissipated in extending the existing debonding region(s), creating additional interfacial debonding, pulling the fibers out of the matrix and producing thickness-direction cracks. The impact tests intermittently were stopped to observe the failure modes of the specimen using SEM and optical microscope. Both of the size and number of delamination cracks as well as thickness-direction cracks were indeed found to increase as the impacts were repeated, figs.7 and 8. These cracks were formed preferentially near the mid-span where the normal stresses are maximal and together they were found to cut more than halfway through the cross-section of the specimen at the late stage of repeated impact testing for all values of E_{inc}. This was consistent with the observations obtained from the static short-beam loading-unloading cycle tests. According to refs. [15,16], a suddenly increased out-of-plane normal stress as a result of matrix cracking was found to predominate the propagation stage of delamination during a single impact event. The same arguments should also be true when considering the growth of interfacial debonding and thickness-direction cracks upon repeated impacts. Ref. [17] reported a continuing reduction in both tensile and compressive strength of carbon/epoxy composites when an increasing number of impacts were imposed on the materials prior to tensile or compressive testing.

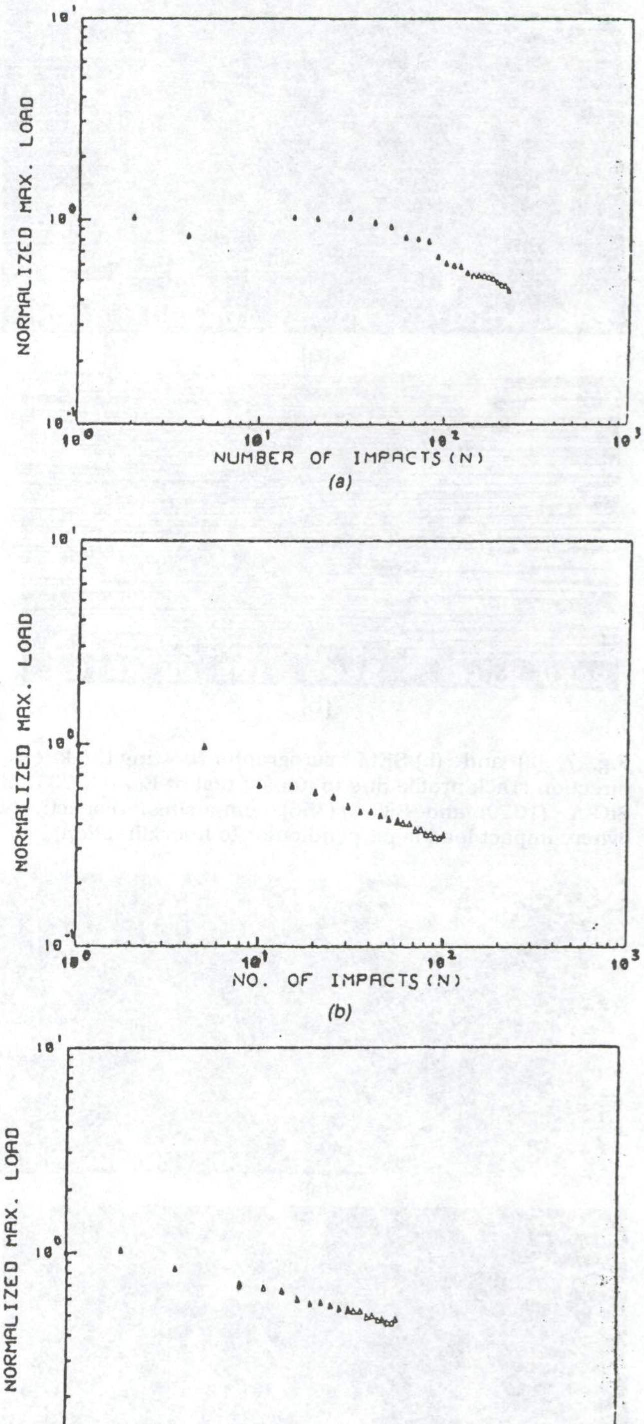

Fig. 6. Normalized maximum load, $\log_{10}\left(P^{N}_{max}/P^{0}_{max}\right)$ vs. number of impacts for SiC- Al(1050) (a) E_{inc} = 4.97J, (b) E_{inc} = 12 J, and C-A1(356) (c) E_{inc} = 7.45 J.

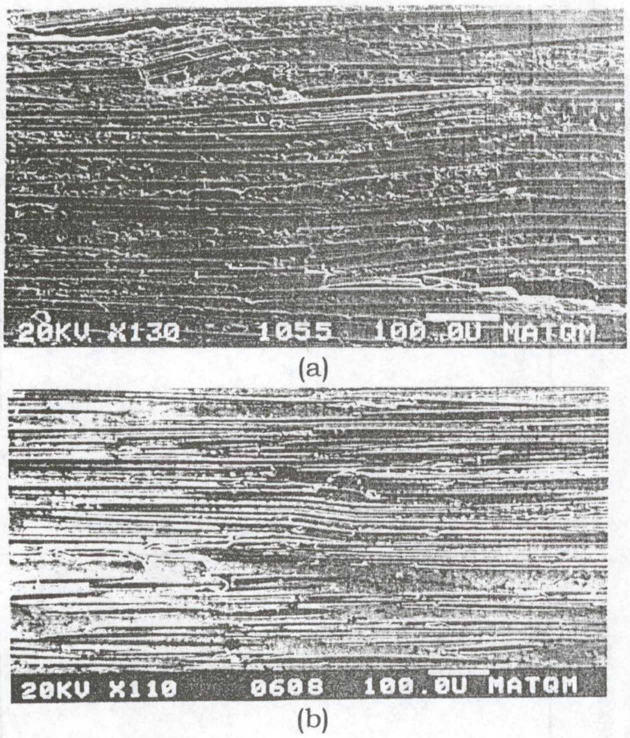

(a)

(b)

Fig. 7. (a) and (b) SEM micrographs showing thickness-direction crack profile due to impact test at E_{inc} = 2.93 J of SiC-A (1050) and SiC-A1(356) composites, respectively (where impact load is perpendicular to fiber direction).

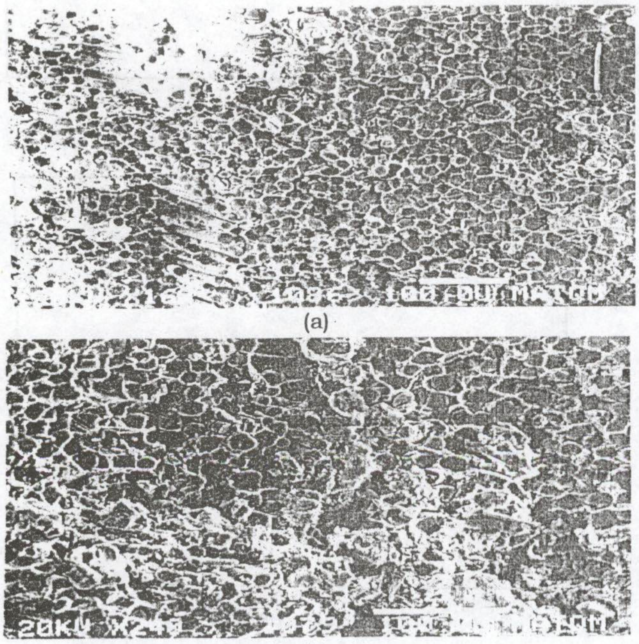

(a)

(b)

Fig. 8. SEM micrographs showing impact fracture surfaces of (a) SiC-A1(1050) composite, (b) SiC-A1(354) composite.

4. Conclusions

The number of impact testing method and the impact failure modes of continuous fiber-reinforced Al-matrix composites have been experimentally investigated. This study has led to the following conclusions.

1) The number of impact(s) tests has been found to be a convenient method for assessing the damage failure tolerance of unidirectionally fiber reinforced metal matrix composites.

2) Matrix cracking is found to be the initial failure mode of impact damage.

3) For a given composite, there exists a threshold incident energy above which significant damage, initiation of delaminations and micro-cracks will occur.

4) Interlaminar shear strength and inplane tensile strength are the dominant factors causing the initial failure mode of matrix cracks.

5) Inplane transverse tensile stress and interlaminar shear stress near matrix cracks produce micro-cracks as delamination (i.e. fiber-matrix interfacial debonding propagates).

6) The impact resistance of SiC-Al (1050) composite, where low fiber-matrix interfacial strength exists, is higher than that of both SiC-Al (354) and C-Al (356) composites that is when the impact load is perpendicular to fiber direction.

Nomenclature

b, d, l	is the Breadth, depth, and span of rectangular beam, respectively,
E_c	Minimum incident energy,
E_{inc}	is the Incident impact energy,
E_m	is the Energy absorbed up to maximum load,
N	is the Number of impacts,
P	is the Load applied to the beam,
P_m^N	is the Maximum load recorded at the Nth. Impact, and
S	is the Elastic modulus of an isotropic beam.

References

[1] H. Chai, W. G. Knauss, and C. D. Babcock, Observation of damage growth in compressively loaded laminates, Exp Mech, Vol. 23, pp. 329-37 (1983).

[2] C. T. Sun, and J. K. Chen, On the impact of initially stressed composite laminate, J Compos Mater, Vol. 19, pp. 490-504 (1985).

[3] G. A. O. Davies, X. Zhang, and A. Edlund, Predicting damage in composite aircraft structures due to low velocity impact, Aerotech'94, Birmingham, UK, January (1994).

[4] J. H. Starnes Jr, M. D. Rhodes, and J. G. Williams, Effect of impact damage and holes on the compressive strength of a graphite/epoxy laminate. Non-destructive evaluation and flaw criticality for composite materials, ASTM STP, Vol. 696, pp. 145-171 (1979).

[5] M. T. Takemori, Biaxial Impact Fatigue of Polycarbonate, J. Materials Science, Vol. 17, pp. 164-172 (1982).

[6] A. S. Prank, and V. P. Tamuzs, Fiber-Glass Laminate Failure Fatigue under the Effect of Repeated Shock Load, Mekh. Polimerov, Vol. 4, pp. 195-199 (1969).

[7] C. Lhymn, Impact Fatigue of PPS/Glass Composites-Theoretical Analysis, J of Materials Sci. Letter, Vol. 4 (1985).

[8] C. Lhymn, Impact Fatigue of PPS/Glass Composites-Microscopy, J of Materials Sci. Letter, Vol. 4, pp. 1429-1433 (1985).

[9] C. Williams, and K. M. Fisher, Solidification Technology in the Foundry and Cast House, The Metals Soc., p.137 (1983).

[10] A. R. Champion, W. H. Krueger, A. S. Hartman, and A. K. Dhinga, Fiber Reinforced Metal Matrix Composites, ICCM-2, TMS, pp. 883-904 (1978).

[11] A. R. Chapman, V. D. Scott, and R. L. Trumper, The Effect of Manufacturing Defects and Second Phases on the Mechanical Behaviour of an Al-Si Alloy Reinforced with Nicalon Fibers, Proc. Conf. ECCM4, Stuttgart, W. Germany, Sept., p.345 (1990).

[12] A. R. Skinner, The effect of heat treatment on the mechanical properties and microstructure of Al-alloy MMC's, Metal Matrix Composites. 2nd Conf. (1989).

[13] B. Z. Jang, L. C. Chen, C. Z. Wang, H. T. Lin, and R. H. Zee, Impact Resistance and Energy Absorption Mechanisms in Hybrid Composites, Composite Science and Technology, Vol. 34, pp. 305-335 (1989).

[14] W. S. Johson, and R. R. Wallis, Fatigue behaviour of continuous fiber Silicone Carbide/Aluminium composites, Composite Materials: Fatigue and Fracture, ASTM STP907, H.T.Hahn, Ed., American Society for Testing and Materials.

[15] F. J. Guild, P. J. Hogg, and J. C. Prichard, A model for the reduction in compression strength of continuous fiber composites after impact damage, Composites, Vol. 24, pp. 333-339 (1993).

[16] H. Y. Choi, and F. K. Chang, A model for predicting damage in graphite/epoxy laminated composites resulting from low-velocity point impact, J Compos Mater, Vol. 26, pp. 2134-69 (1992).

[17] X. Zhang, G. A. O. Davies, and D. Hitchings, Impact damage with compressive preload and post-impact compression of carbon composite plates, International Journal of Impact Engineering, Vol. 22, pp. 485-509 (1999).

Received April 4, 2001
Accepted December 25, 2001